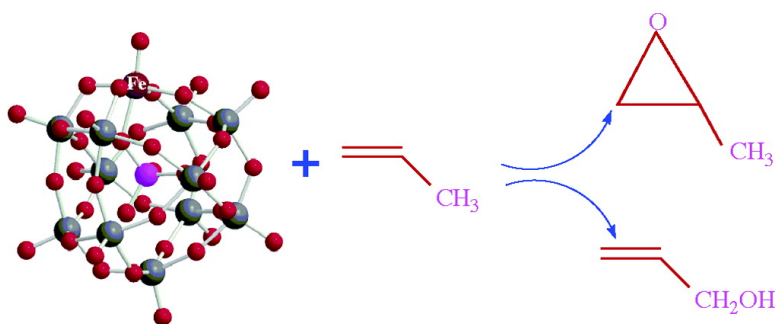


The High-Valent Iron–Oxo Species of Polyoxometalate, if It Can Be Made, Will Be a Highly Potent Catalyst for C–H Hydroxylation and Double-Bond Epoxidation

Devesh Kumar, Etienne Derat, Alexander M. Khenkin, Ronny Neumann, and Sason Shaik

J. Am. Chem. Soc., **2005**, 127 (50), 17712-17718 • DOI: 10.1021/ja0542340 • Publication Date (Web): 19 November 2005

Downloaded from <http://pubs.acs.org> on March 25, 2009



More About This Article

Additional resources and features associated with this article are available within the HTML version:

- Supporting Information
- Links to the 12 articles that cite this article, as of the time of this article download
- Access to high resolution figures
- Links to articles and content related to this article
- Copyright permission to reproduce figures and/or text from this article

[View the Full Text HTML](#)

The High-Valent Iron–Oxo Species of Polyoxometalate, if It Can Be Made, Will Be a Highly Potent Catalyst for C–H Hydroxylation and Double-Bond Epoxidation

Devesh Kumar,[†] Etienne Derat,[†] Alexander M. Khenkin,[‡] Ronny Neumann,^{*,‡} and Sason Shaik^{*,†}

Contribution from the Department of Organic Chemistry and the Lise Meitner-Minerva Center for Computational Quantum Chemistry, The Hebrew University, Jerusalem, 91904, Israel, and Department of Organic Chemistry, Weizmann Institute of Science, Rehovot, 76100 Israel

Received June 27, 2005; E-mail: sason@yfaat.ch.huji.ac.il.

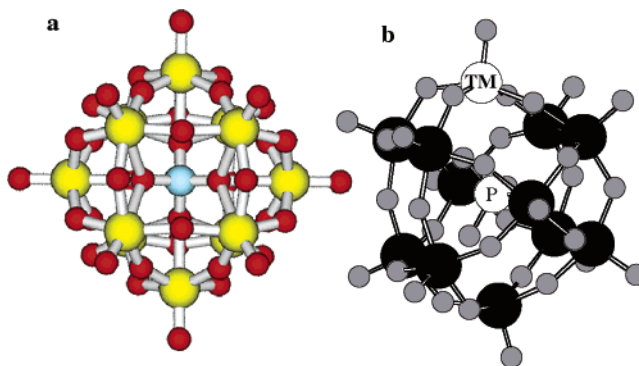
Abstract: This study uses density functional theory (DFT) calculations to explore the reactivity of the putative high-valent iron–oxo reagent of the iron-substituted polyoxometalate (POM–FeO⁴⁻), derived from the Keggin species, PW₁₂O₄₀³⁻. It is shown that POM–FeO⁴⁻ is in principle capable of C–H hydroxylation and C=C epoxidation and that it should be a powerful oxidant, even more so than the Compound I species of cytochrome P450. The calculations indicate that in a solvent, the barriers, and especially those for epoxidation, become sufficiently small that one may expect an extremely fast reaction. An experimental investigation (by R.N. and A.M.K.) shows, however, that the formation of POM–FeO⁴⁻ using the oxygen donor, F₅PhI–O, leads to a persistent adduct, POM–FeO–I–PhF₅⁴⁻, which does not decompose to POM–FeO⁴⁻ + F₅Ph–I at the working temperature and exhibits sluggish reactivity, in accord with previous experimental results (Hill, C. L.; Brown, R. B., Jr. *J. Am. Chem. Soc.* **1986**, *108*, 536 and Mansuy, D.; Bartoli, J.-F.; Battioni, P.; Lyon, D. K.; Finke, R. G. *J. Am. Chem. Soc.* **1991**, *113*, 7222). Subsequent calculations indeed reveal that the gas-phase binding energy of F₅PhI to POM–FeO⁴⁻ is high (ca. 20 kcal/mol) compared to the corresponding binding energy of propene (ca. 2–3 kcal/mol). As such, the POM–FeO–I–PhF₅⁴⁻ complex is expected to be persistent toward the displacement of F₅PhI by a substrate like propene, leading thereby to sluggish oxidative reactivity. According to theory, overcoming this technical difficulty may turn out to be very rewarding. The question is, can POM–FeO⁴⁻ be made?

Introduction

Polyoxometalates (POMs) constitute a diverse class of inorganic oxo–metal clusters with defined structures based on octahedra of tungstic and/or molybdic oxides, e.g., the PW₁₂O₄₀³⁻ Keggin type species in Scheme 1a, which possesses a central phosphate moiety that coordinates the edge-sharing WO₆ octahedra into a single cluster.¹ The stability of these compounds to strongly oxidizing conditions has made POMs extremely attractive as oxidation catalysts and for activation of environmentally benign oxidants.²

An important subgroup of polyoxometalate compounds are those so-called transition metal (TM)-substituted polyoxometalates (POM–TM) where transition metals are inserted into a lacunary or defect position of the polyoxometalate. It has been suggested that such compounds may be viewed as transition metal complexes with an inorganic polyoxometalate ligand that

Scheme 1



^a The PW₁₂O₄₀³⁻ species. The central atom in blue is phosphorus, the larger circles in yellow are tungstens, and the small red circles are oxygens.

^b A schematic representation of a [PW₁₂O₃₉]TM=O species made from the PW₁₂O₄₀³⁻ species.

acts as a potential multielectron acceptor.² An especially intriguing aspect of POM–TMs has been the activation of these complexes with oxygen donors, which thereby elicit catalytic activity toward double-bond epoxidation and C–H hydroxylation. A significant number of such applications have appeared in the literature, including reversible dioxygen complexation to a POM–Mn(II),³ activation of dioxygen by a POM–Ru(II)

[†] The Hebrew University.

[‡] Weizmann Institute of Science.

- (1) (a) Pope, M. T. *Isopoly and Heteropoly Anions*; Springer: Berlin, 1983. (b) Pope, M. T.; Müller, A., Eds., *Polyoxometalate Chemistry*; Kluwer Academic: Dordrecht, The Netherlands, 2001.
- (2) (a) Kozhevnikov, I. V. *Catalysis by Polyoxometalates*; Wiley: Chichester, England, 2002. (b) Hill, C. L.; Prosser-McCartha, C. M. *Coord. Chem. Rev.* **1995**, *143*, 407. (c) Mizuno, N.; Misono, M. *Chem. Rev.* **1998**, *98*, 199. (d) Neumann, R. *Prog. Inorg. Chem.* **1998**, *47*, 317.

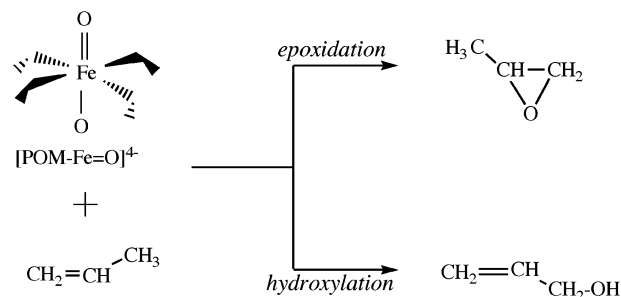
complex,⁴ activation of monooxygen donors such as iodosobenzene,⁵ nitrous oxide,⁶ and others⁷ by various POM–TMs.

It has been generally assumed that the activation of these POM–TM complexes by oxygen atom donors such as iodosobenzene leads to the high-valent POM–TM=O species, e.g., in Scheme 1b,⁵ analogous to the Compound I species of heme enzymes,^{8,9} and to synthetic Compound I-like catalysts.¹⁰ Thus, it was reported that POM–Mn(III) catalyzes oxygen transfer reactions from iodosobenzene to alkenes and alkanes in a manner (activity, selectivity) similar to what has been observed for analogous metalloporphyrins.⁵ By contrast, the corresponding POM–Fe(III) was reported to be a very sluggish catalyst, leading to meager oxygen transfer activity to organic substrates.⁵ This latter result is intriguing in view of the high reactivity of iron–oxo porphyrin species^{8,9,10a} as well as of nonheme iron–oxo catalysts.^{10b–d} Is this sluggishness of the POM–Fe(III) complex rooted in the lack of reactivity of the corresponding iron–oxo complex, POM–Fe=O? This is the central question dealt with in the present contribution by theoretical and experimental means.

In a recent communication,¹¹ we presented density functional theory (DFT) results for the POM–Fe=O^{4–} and the oxidized form, POM–Fe=O^{3–}. The electronic structure of these complexes revealed the apparent similarity, albeit with some differences, to the corresponding Compound I species of the enzyme P450. While some rationalization was attempted to account for the apparent sluggishness of these proposed species as oxygenating agents, it was at the same time clear that this question merited an eventual direct study of C–H hydroxylation and double-bond epoxidation by POM–Fe=O^{4–}. Thus, a complete DFT study of the hydroxylation and epoxidation of propene by PW₁₁O₃₉Fe=O^{4–} was carried out. Simultaneously, an attempt was made to experimentally probe the formation and reactivity of the proposed POM–Fe=O species. The present contribution describes these studies.

The two processes that were studied by DFT calculations are summarized in Scheme 2. Propene was chosen as a substrate since it contains both C=C and C–H oxidizable moieties, and because these reactions can be compared to the same ones

Scheme 2. Theoretically Studied Epoxidation and Hydroxylation Processes of Propene by POM–Fe=O^{4–}



studied previously using Compound I of P450.¹² Experimentally, the formation of POM–Fe=O^{4–} was studied (by R.N. and A.M.K.) by employing commonly used monooxygen donors to transition metals, iodosobenzene, PhI=O,^{10a} and iodosopentafluorobenzene, F₅PhI=O. As shall be demonstrated by calculations, POM–Fe=O^{4–} is a powerful oxidant, more so than Compound I of P450. However, this intermediate was experimentally inaccessible; instead a nonreactive and stable POM–Fe–O–IAr complex is formed.

Methods

Theoretical Procedures. Following the previous study,¹¹ here too the [PW₁₁O₃₉Fe=O]^{4–} species was generated from [PW₁₂O₄₀]^{3–} by replacing a single [W^{VI}=O]⁴⁺ group by [Fe^V=O]³⁺. The oxidation state of the iron (V) corresponds to the same effective oxidation state of Compound I species, in which Fe^{IV}=O is coordinated to a porphyrin radical cation.^{8–10a} Since the truncation of [W^{VI}=O]⁴⁺ leaves behind a lacunary [PW₁₁O₃₉]^{7–}, the combination of this lacunary with the [Fe^V=O]³⁺ fragment generates the [PW₁₁O₃₉Fe=O]^{4–} species with a total charge of 4–. The starting geometry was the neutron diffraction structure¹³ of [PW₁₂O₄₀]^{3–} into which the Fe=O moiety was inserted, by the above-described replacement. The so resulting structure was calculated by DFT using the unrestricted hybrid functional, UB3LYP,¹⁴ and the double- ζ effective core potential basis set, LANL2DZ.¹⁵ Subsequently, the structure was optimized at the UB3LYP/LANL2DZ level, implemented in GAUSSIAN98,^{16a} and the very similar level UB3LYP/LACVP, implemented in JAGUAR5.5.^{16b} Since the two structures were virtually identical (see Figure 1, later), we preferred to use UB3LYP/LACVP, due to the greater speed of JAGUAR, compared with GAUSSIAN, in geometry optimization procedures. DFT calculations of POM derivatives are gradually appearing more frequently in the current literature,¹⁷ and the overall impression is that the method is not only a pragmatic one, but that its results seem also quite reliable.¹⁷ⁱ

- (3) Katsoulis, D. E.; Pope, M. T. *J. Am. Chem. Soc.* **1984**, *106*, 2737.
 (4) (a) Neumann, R.; Dahan, M. *Nature* **1997**, *388*, 353. (b) Neumann, R.; Dahan, M. *J. Am. Chem. Soc.* **1998**, *120*, 11969.
 (5) (a) Hill, C. L.; Brown, R. B., Jr. *J. Am. Chem. Soc.* **1986**, *108*, 536. (b) Mansuy, D.; Bartoli, J.-F.; Battioni, P.; Lyon, D. K.; Finke, R. G. *J. Am. Chem. Soc.* **1991**, *113*, 7222.
 (6) (a) Ben-Daniel, R.; Weiner, L.; Neumann, R. *J. Am. Chem. Soc.* **2002**, *124*, 8788. (b) Ben-Daniel, R.; Neumann, R. *Angew. Chem., Int. Ed.* **2003**, *42*, 92.
 (7) (a) Zhang, X.; Sasaki, K.; Hill, C. L. *J. Am. Chem. Soc.* **1996**, *118*, 4809. (b) Neumann, R.; Abu-Gnim, C. *J. Am. Chem. Soc.* **1990**, *112*, 6025. (c) Neumann, R.; Khenkin, A. M. *Chem. Commun.* **1998**, 1967.
 (8) (a) Ortiz de Montellano, P. R., Ed. *Cytochrome P450: Structure, Mechanism and Biochemistry*, 2nd ed.; Plenum Press: New York, 1995. (b) Ortiz de Montellano, P. R., Ed. *Cytochrome P450: Structure, Mechanism and Biochemistry*, 3rd ed.; Kluwer Academic/Plenum Publishers: New York, 2004. (c) Poulos, T. L. In *The Porphyrin Handbook*; Kadish, K. M., Smith, K. M., Guilard, R., Eds.; Academic Press: New York, 2000; Vol. 4, p 190. (d) Groves, J. T. *Proc. Natl. Acad. Sci. U.S.A.* **2003**, *100*, 3569. (e) Sono, M.; Roach, M. P.; Coulter, E. D.; Dawson, J. H. *Chem. Rev.* **1996**, *96*, 2841.
 (9) Harris, D. L. *Curr. Opin. Chem. Biol.* **2001**, *5*, 724.
 (10) (a) Groves, J. T.; Han, Y.-Z. In *Models and Mechanisms of Cytochrome P450 Action*; Chapter 1, p 3 in ref 8(a). (b) Costas, M.; Mehn, M. P.; Jensen, M. P.; Que, L., Jr. *Chem. Rev.* **2004**, *104*, 939. (c) Kaizer, J.; Klinker, E. J.; Oh, N. Y.; Rohde, J.-U.; Song, W. J.; Stubna, A.; Kim, J.; Münck, E.; Nam, W.; Que, L., Jr. *J. Am. Chem. Soc.* **2004**, *126*, 472. (d) Rohde, J.-U.; In, J.-H.; Lim, M. H.; Brennessel, W. W.; Bukowski, M. R.; Münck, E.; Nam, W.; Que, L., Jr. *Science* **2003**, *299*, 1037.
 (11) de Visser, S. P.; Kumar, D.; Neumann, R.; Shaik, S. *Angew. Chem., Int. Ed.* **2004**, *43*, 5661.

- (12) de Visser, S. P.; Ogliaro, F.; Sharma, P. K.; Shaik, S. *J. Am. Chem. Soc.* **2002**, *124*, 11809.
 (13) Brown, G. M.; Noe-Spirlet, M. R.; Busing, W. R.; Levy, H. A. *Acta Crystallogr., Sect. B* **1977**, *34*, 1038.
 (14) (a) Becke, A. D. *J. Chem. Phys.* **1992**, *96*, 2155. (b) Becke, A. D. *J. Chem. Phys.* **1992**, *97*, 9173. (c) Becke, A. D. *J. Chem. Phys.* **1993**, *98*, 5648. (d) Lee, C.; Yang, W.; Parr, R. G. *Phys. Rev. B* **1988**, *37*, 785.
 (15) Dunning, T. H., Jr.; Hay, P. J. In *Modern Theoretical Chemistry*; Schaefer, H. F., III, Ed.; Plenum: New York, 1976; pp 1–28.
 (16) (a) Frisch, M. J.; et al. *Gaussian 98*; Gaussian, Inc.: Pittsburgh, PA, 1998. (b) *Jaguar 5.5*; Schrödinger, Inc.: Portland, OR, 2003.
 (17) See for example: (a) Bagno, A.; Bonchio, M.; Sartorel, A.; Scorrano, G. *ChemPhysChem* **2003**, *4*, 517. (b) Maestre, J. M.; Lopez, X.; Bo, C.; Poblet, J.-M.; Casan-Pastor, N. *J. Am. Chem. Soc.* **2001**, *123*, 3749. (c) Tsiapis, A.; Tsiapis, C. A. *J. Phys. Chem. A* **2000**, *104*, 859. (d) Rohmer, M.-M.; Bénard, M.; Cadot, E.; Secheresse, F. In *Polyoxometalate Chemistry*; Pope, M. T., Müller, A., Eds.; Kluwer Academic Publishers: The Netherlands, 2001; p 117. (e) Duclausaud, H.; Boshch, S. A. *Inorg. Chem.* **1999**, *38*, 3489. (f) Duclausaud, H.; Boshch, S. A. *J. Am. Chem. Soc.* **2001**, *123*, 2825. (g) Bridgeman, A. *Chem. Eur. J.* **2004**, *10*, 2935. (h) Musaev, D. G.; Morokuma, K.; Geletii, Y. V.; Hil, C. L. *Inorg. Chem.* **2004**, *43*, 7702. For a recent interplay of DFT and experiment, see: (i) Anderson, T. M.; Neiwert, W. A.; Kirk, M. L.; Piccoli, P. M. B.; Schultz, A. J.; Koetzle, T. E.; Musaev, D. G.; Morokuma, K.; Cao, R.; Hill, C. L. *Science* **2004**, *306*, 2074.

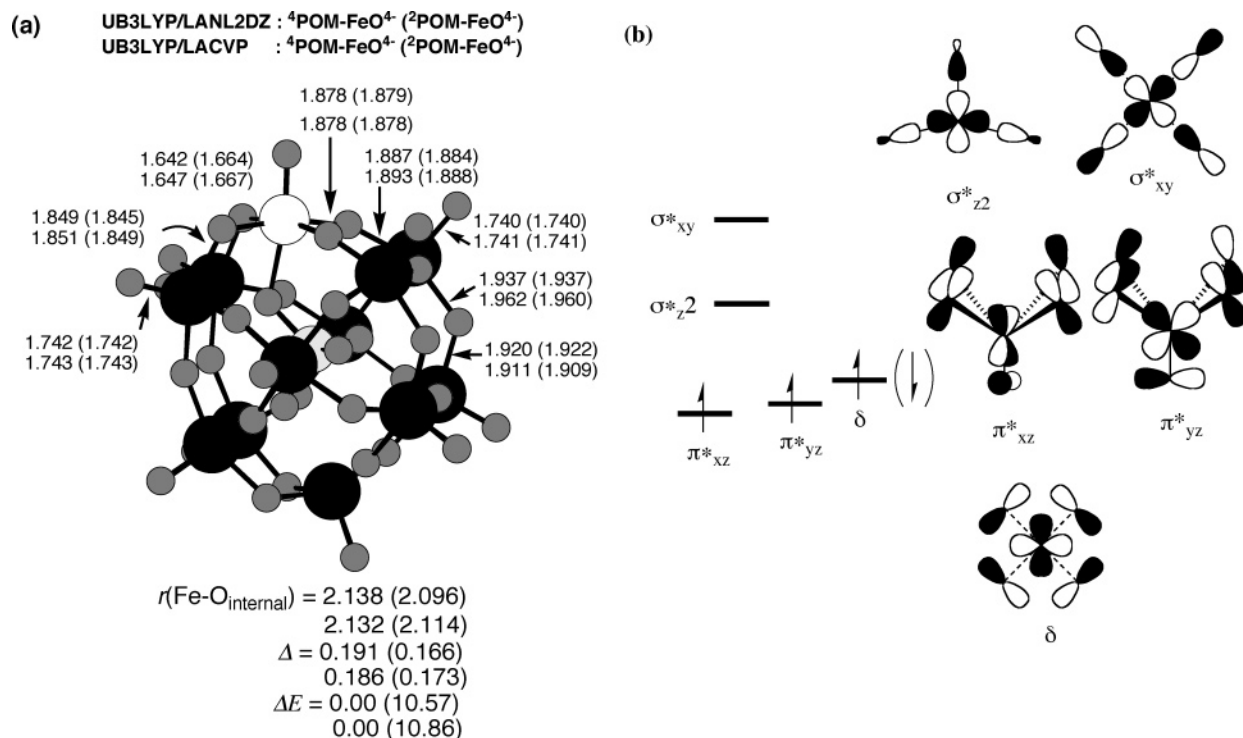


Figure 1. Optimized geometries and relative energies (a) and electronic structure (b) of POM-FeO^{4+} in the quartet and doublet states. Each geometric (energy) value is presented in two lines; the upper line corresponds to UB3LYP/LANL2DZ values, the lower to UB3LYP/LACVP values. The relative energies, ΔE , are in kcal/mol, and the distances are in angstroms.

All the geometries were optimized with JAGUAR 5.5. In the cases of **1** and the transition states the structures were verified by frequency calculations, using GAUSSIAN98 (at the UB3LYP/LACVP level), which has a more robust and faster frequency calculation routine. Since frequency calculations for these systems take extremely long time, the rest of the frequency calculation had to be waived. Reaction pathways were verified by a scan along a given coordinate, while optimizing freely all other coordinates. Single-point calculations were carried out, on the optimal species, with the larger basis set, LACV3P⁺⁺(iron)/6-311+G*(rest), for energy evaluation.^{16b} Similar single-point calculations were done on the respective species, in ref 12, for the reaction of P450 Compound I with propene. Hereafter, we refer to LACVP as B1 and to LACV3P⁺⁺ as B2.

The effect of solvent was systematically estimated using the SCRF model, based on the Poisson–Boltzmann equation, as implemented in JAGUAR5.5; this model defines the solvent by two parameters, a dielectric constant (ϵ) and a probe radius (r); the program calculates the cavity of the solute.^{16b} Since ionic solvation varies in proportion to the square of the ionic charge, then any small inaccuracy in the model (e.g., solvent parameters or calculation of the cavity of the solute) will be highly amplified for a quadruply charged species such as POM-FeO^{4+} . To avoid this pitfall as much as possible we used two different sets of solvent parameters: one is the commonly used solvent in our theoretical studies of P450 reactions,¹² with $\epsilon = 5.7$ and $r = 2.7$ Å, the other being more polar with $\epsilon = 37.5$ (as for acetonitrile), $r = 2.2$ Å. In a few of the cases (the complex of POMFeO^{4+} with $\text{F}_5\text{C}_6\text{I}$) we employed also the model COSMO implemented in GAUSSIAN03.^{16a,18} We must, however, emphasize that what matter are the trends relative to the gas phase rather than the absolute quantitative results in the solvents.

The data are summarized in the Supporting Information deposited with this paper, while the text focuses on the key results.

Results and Discussion

Structures and Electronic Features of POM-Fe=O^{4+} . As shown in a previous theoretical study,¹¹ POM-Fe=O^{4+} , **1**, possesses two triradicaloid states with three unpaired electrons; a quartet ground state followed by a doublet state, hence 4^21 . The optimized geometries of these states are shown in Figure 1a and the corresponding electronic structures in Figure 1b. Figure 1a shows that the optimal values determined with LANL2DZ and LACVP are, as expected, very similar. A few features are notable: first, the Fe=O distances of 1.64–1.66 Å are very similar to the average distance reported for many Compound I species of heme enzymes,^{8c,9,19} synthetic porphyrin iron–oxo models,^{8d,10a} and nonheme iron–oxo compounds.^{10b–d} Second, compared to the electron diffraction structure of the pristine POM,¹³ where the distance between tungsten and the oxygen ligand of the phosphaste group, $r(\text{W-O}_{\text{internal}})$, is 2.437 Å, the corresponding distance in the case of iron, $r(\text{Fe-O}_{\text{internal}})$, is considerably shorter, ca. 2.1 Å. Indeed, all other Fe-O distances are shorter than the corresponding W-O distances, and as such, the replacement of W=O by Fe=O causes some distortion of the cage as though FeO pinches the $\text{PW}_{12}\text{O}_{39}$ lacunary. Finally, as shown by the Δ parameter, the Fe atom deviates from the mean plane of the close coordinate shell (Fe-O_4) by 0.19 Å, significantly more than in the case of Compound I of P450.

The electronic structure in Figure 1b shows that the d-block orbitals (for detailed drawings of these and other orbitals see the Supporting Information, Figure S2) split in a three-below-two pattern, typical to hexacoordination. The ground state, 41 ,

(18) Barone, V.; Cossi, M. *J. Phys. Chem. A* **1998**, *102*, 1995.

(19) Shaik, S.; Kumar, D.; de Visser, S. P.; Altun, A.; Thiel, W. *Chem. Rev.* **2005**, *105*, 2279.

involves three electrons in a high-spin occupation of three d-type orbitals, π^* and δ . In the higher doublet state, the spin of the δ electron is opposite to the ones of the π^* electrons. The energy difference between the two spin states is significant, 10.9/13.2 kcal/mol with B1/B2, and reflects the stabilization of the quartet state by two additional d–d exchange interactions of the open-shell electronic system. Similar gaps were reported previously with the BP86 pure functional (Table S2 in the Supporting Information),¹¹ so one may consider this energy splitting as being fairly reasonable. Thus, with the $\pi^*1\pi^*1\delta^1$ configuration, the POM–FeO⁴⁻ complex involves a triplet Fe(V)O moiety strongly coupled to a third electron in ferromagnetic (⁴1) and antiferromagnetic (²1) coupling modes. Other states were tested before,¹¹ but all were found to be higher in energy than the ^{2,4}1 pair described here and hence were not considered for the reactivity study.

Stability Patterns of POM–Fe=O⁴⁻. The stability of ⁴POM–FeO⁴⁻ toward one electron oxidation was tested before.¹¹ It was shown that in the gas phase the species loses an electron spontaneously (IP = –23.5 kcal/mol) but in a solvent (using COSMO and a dielectric constant of water¹¹) the ionization potential was quite significant, IP = +169.5 kcal/mol (oxidation potential = +2.8 V relative to the standard hydrogen electron (SHE)). Addition of an electron to ⁴POM–FeO⁴⁻ generates the species ^{3,5}POM–FeO⁵⁻, which in the gas phase will lose an electron spontaneously (IP = –139.4/–134.7 kcal/mol for the triplet/quintet states). The use of the SCRf model in JAGUAR^{16b} leads to positive values IP = +104.5/+100.0 kcal/mol for a dielectric constant of 5.7 and +139.4/+134.7 kcal/mol for a dielectric constant of 37.5 (corresponding to oxidation potentials = –0.017/–0.212 V and +1.469/+1.292 V relative to SHE). We may therefore conclude that in the presence of strong reducing reagents, with IP < 130 kcal/mol, the POM–FeO⁴⁻ reagent will be reduced to POM–FeO⁵⁻. The ionization potential of propene, the substrate used in this study, is 224.4 kcal/mol,²⁰ and in a solvent it will be approximately 170 kcal/mol (solvation energies of monocationic carbon cations are ca. 50 kcal/mol). Thus, propene will not transfer an electron to POM–FeO⁴⁻ and is therefore an appropriate substrate for the present study.

Epoxidation of Propene by POM–Fe=O⁴⁻. The reaction profile for the epoxidation of propene is depicted in Figure 2, while the geometries of the critical species are drawn in Figure 3. The reaction starts from initial reaction clusters, ^{4,2}RC, which are weakly stabilized relative to the reactants. This is followed by the corresponding transition states of bond activation, ^{4,2}TS1, which lead to two intermediates, ^{4,2}2, which subsequently undergo ring closure via two transition states, ^{4,2}TS2, terminating at the ferric epoxide product complexes, ^{4,2}3. The mechanism resembles very much the corresponding one for epoxidation by Compound I of P450 species.¹²

Figure 2 exhibits two interesting new features. The first one is the shrinkage of the doublet–quartet gap, which starts as 9 kcal/mol or so in favor of the quartet state, and reduces to 1 kcal/mol at the intermediate, ^{4,2}2, stage. This change reflects a corresponding change in the electronic structure. Thus, in ^{4,2}1,

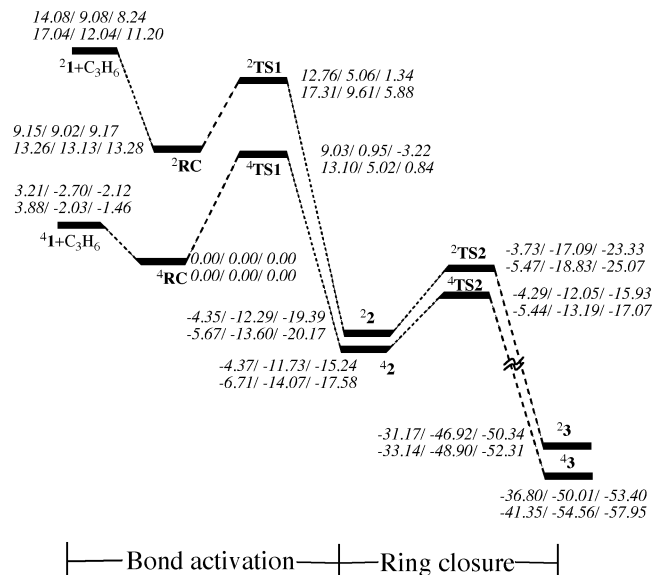


Figure 2. Energy profile for the epoxidation mechanism of propene by ^{4,2}1. The energies (in kcal/mol) of each species, relative to the quartet reaction complex ⁴RC, are given in two lines. The upper line gives UB3LYP/B1 energies, while the lower line lists UB3LYP/B2 energies. In each line there are three entries $\Delta E/\Delta E(\epsilon = 5.7)/\Delta E(\epsilon = 37.5)$ corresponding to energy only and energy with the solvation corrections for the two solvents used in the study. The corresponding geometries are given in Figure 3.

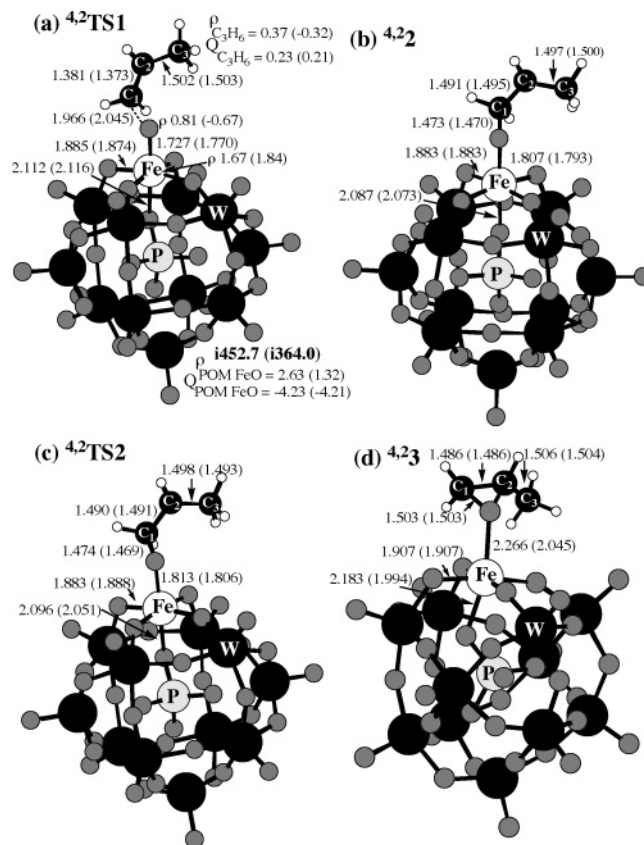


Figure 3. Key geometric features of the critical species along the epoxidation pathway described in Figure 2: (a) bond activation transition states, ^{4,2}TS1, (b) ^{4,2}2 intermediates, (c) ring closure transition states, ^{4,2}TS2, and (d) ^{4,2}3 epoxide complexes. Some spin (ρ) and charge (Q) densities are indicated near the species. Distances are in angstroms.

(20) The IP of propene in the gas phase is 224.4 kcal/mol, see: (a) Traeger, J. C. *Int. J. Mass Spectrom. Ion Processes* **1984**, *58*, 259. For the effect of solvent on IP of, e.g., allyl cation, see: (b) Shaik, S.; Cohen, S.; de Visser, S. P.; Sharma, P. K.; Kumar, D.; Kozuch, S.; Oglario, F.; Danovich, D. *Eur. J. Inorg. Chem.* **2004**, 207.

intermediate, the iron–hydroxo complex has only two unpaired electrons, while the third one is located on the propene moiety; now the coupling between the d-orbitals and the propene-centered orbital is weak, and hence the quartet–doublet splitting becomes very small, similar to the situation in P450.^{12,19}

The second interesting feature is the remarkably small barriers for bond activation, which becomes even smaller when solvation correction is added. The reason for this solvent effect is the electrophilic nature of the iron–oxo moiety. As a result of this nature, some electron density is transferred from the propene to the iron–oxo, and as such the negative charge on the POM–FeO moiety increases compared with the charge on the reactant, POM–FeO⁴⁺ or the reaction complex, RC, and some positive charge builds up on the propene (see Figure 3 below). Since the POM–FeO moiety is quadruply charged and ionic solvation is proportional to the square of the charge, the increase of the negative charge on the POM–FeO moiety will create a heightened sensitivity to solvent effect. The consequence of these changes in charge density is the better solvation of ^{4,2}TS1 compared with the reactants (^{4,2}1 + C₃H₆) and the reaction complexes, ^{4,2}RC, and hence, reduction of the bond activation barriers relative to the gas-phase values. The resulting small barriers (7.1/2.3 kcal/mol for the B2 data with $\epsilon = 5.7/\epsilon = 37.5$) are in apparent contradiction with experimental data, where the iron species appears unreactive as an oxidant.⁵ As shall be seen later there is a good reason for the apparent disparity between theory and experiment.

Figure 3 depicts the structures of the critical species, along with some spin density (ρ) and charge density (Q) data. Thus, compared with **1**, the bond activation TS1 species exhibit some elongation of the Fe–O and C=C bonds, which participate in the activation. A significant amount of spin density is transferred to the propene and is concentrated mostly on C2 (0.59 in ^{4,2}TS1 and –0.55 in the ²TS1). The spin density transfer is attended by charge density depletion on the propene that acquires a significant positive charge, +0.23 (+0.21). These changes become more significant in the intermediates, ^{4,2}2, where now the spin density on the propene is close to 1.0 and the O–C bond is fully made. The ring closure transition states, ^{4,2}TS2, exhibit the expected decrease of the spin density on the propene moiety. The epoxide product complexes, ^{4,2}3, are what one would expect from such ferric complexes, with normal bond lengths and iron spin density of almost 3.0/1.0 for quartet/doublet complexes.

Allylic Hydroxylation of Propene by POM–Fe=O⁴⁺. Figure 4 traces the energy profile for the allylic hydroxylation of propene, while Figure 5 depicts the critical structures. The process follows the rebound mechanism suggested first by Groves and McClusky²¹ for C–H hydroxylation by the Compound I species of P450, but having two reactive states, quartet and doublet. Initially the iron–oxo reagent abstracts a hydrogen atom from the allylic position of propene, leading to an allyl radical coordinated weakly to an iron–hydroxo complex, ^{4,2}4. The allyl radical then rebounds onto the hydroxo group and generates the ferric–alcohol complexes, ^{4,2}5. Here too we witness the same features as in epoxidation; first, the shrinkage of the energy gap between the spin states, which collapse at the intermediate stage, and second, the significant solvent effect that lowers the barrier relative to the gas phase. Thus, here too

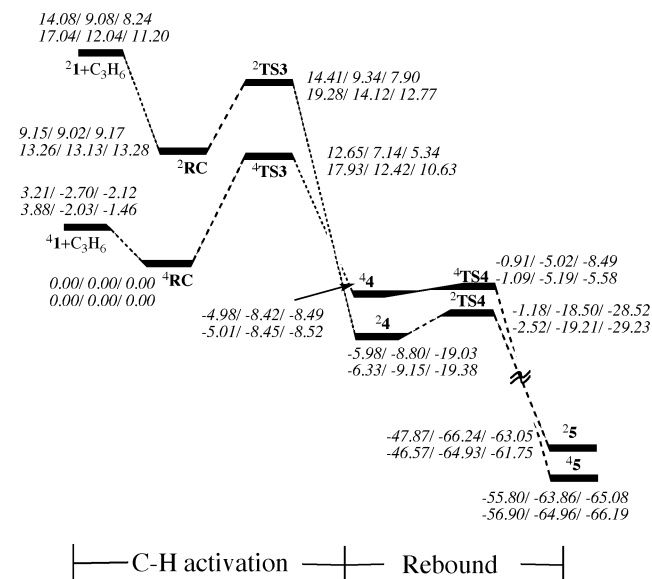


Figure 4. Energy profile for the C–H hydroxylation mechanism of propene by ^{4,2}1. The energies (in kcal/mol) of each species, relative to the quartet reaction complex ⁴RC, are given in two lines. The upper line gives UB3LYP/B1 energies, while the lower line lists UB3LYP/B2 energies. In each line there are three entries labeled as $\Delta E/\Delta E(\epsilon = 5.7)/\Delta E(\epsilon = 37.5)$ that correspond to energy only and energy with solvation corrections for the two solvents used in the study. The corresponding geometries are given in Figure 5.

the barriers are sufficiently small to expect efficient C–H hydroxylation by the POM–FeO⁴⁺ reagent. The structures in Figure 5 show also the same trends in the spin and charge density as in the epoxidation. In general, there is great similarity between the reactivity of POM–FeO⁴⁺ and Compound I of P450.¹²

Experimental Results. As reported in the literature,⁵ also in our hands in this study, iron-substituted polyoxometalates were practically inactive (1–2 turnovers, 12 h) as catalysts for epoxidation of alkenes such cyclooctene using iodosobenzene as oxygen donor. To rely on ³¹P NMR as a probe of the reactivity of an iron-substituted polyoxometalate, we used the iron-substituted Wells–Dawson type polyoxometalate, ⁴Q₇[P₂Fe^{III}(H₂O)W₁₇O₆₁] (⁴Q = *n*-Bu₄N⁺),²² where the phosphorus heteroatoms are not equivalent. The ³¹P NMR of ⁴Q₇[P₂Fe^{III}(H₂O)W₁₇O₆₁] in CD₃CN showed a broadened peak at –14.8 ppm for the phosphorus heteroatom distal to the iron(III) center of the polyoxometalate; the phosphorus atom vicinal to the Fe(III) was not observed due to the paramagnetic effect. Addition of a 5-fold excess pentafluoriodosobenzene, F₅PhIO, at room temperature yielded a similar spectrum with a shifted broad peak at –14.1 ppm. From this experiment one may conclude that a new stable species was formed, which still has a paramagnetic iron center. The UV–vis spectrum of this intermediate species was essentially unchanged from the initial ⁴Q₇[P₂Fe^{III}(H₂O)W₁₇O₆₁] compound, both being yellowish and having a maximum at 242 nm with a broad shoulder at 420 nm. Furthermore, addition of F₅PhIO to ⁴Q₇[P₂Fe^{III}(H₂O)W₁₇O₆₁] showed almost no decomposition of the oxidant over 3 h as determined by iodometric titration of the oxidant. This experiment showed that the intermediate formed as observed by ³¹P NMR was not a reactive intermediate. In a further

(21) Groves, J. T.; McClusky, G. A. *J. Am. Chem. Soc.* **1976**, *98*, 859.

(22) Lyon, D. K.; Miller, W. K.; Novet, T.; Domaille, P. J.; Evitt, E.; Johnson, D. C.; Finke, R. G. *J. Am. Chem. Soc.* **1991**, *113*, 7209.

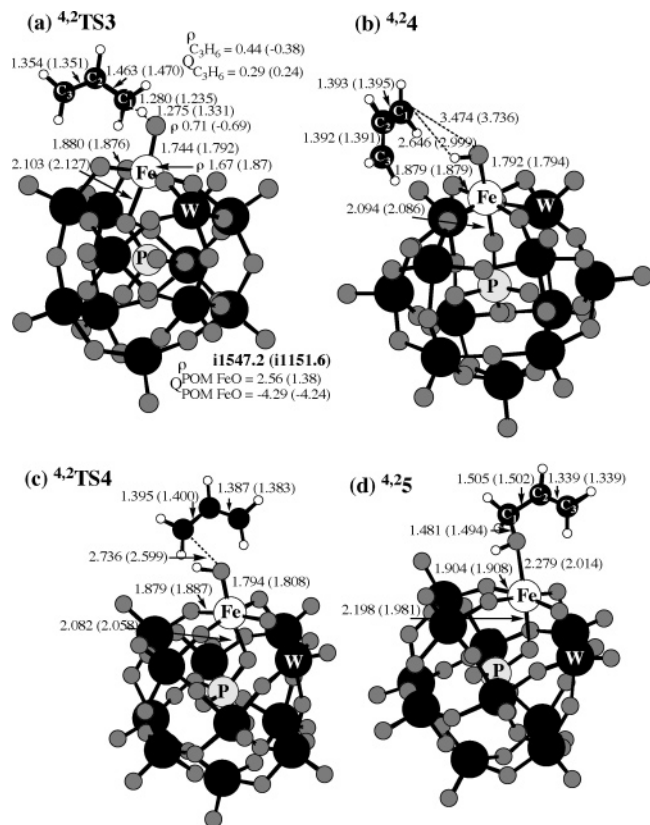


Figure 5. Key geometric features of the critical species along the allylic hydroxylation pathway described in Figure 4; data out of parentheses correspond to the quartet state species, while those in parentheses correspond to the doublet: (a) bond activation transition states, $4,2\text{TS}3$, (b) $4,24$ intermediates, (c) rebound transition states, $4,2\text{TS}4$, and (d) $4,25$ ferric-alcohol complexes. Some spin (ρ) and charge (Q) densities are indicated near the species. Distances are in angstroms.

experiment, 0.5 equiv of F_5PhIO (^{19}F NMR -119.43 , -138.57 , -153.56 ppm) was added to a solution of ${}^4\text{Q}_7[\text{P}_2\text{Fe}^{\text{III}}(\text{H}_2\text{O})\text{W}_{17}\text{O}_{61}]$ in CD_3CN at -50 °C. The ^{19}F NMR changed significantly with peaks at -121.89 , -146.31 , and -157.38 ppm). Upon letting this solution warm to room temperature there was essentially no change in the ^{19}F NMR. Practically no F_5PhI was formed (^{19}F NMR -119.35 , -152.50 , -159.57 ppm). From the combined experiments described, one may reasonably conclude that the addition of oxygen surrogates to ${}^4\text{Q}_7[\text{P}_2\text{Fe}^{\text{III}}(\text{H}_2\text{O})\text{W}_{17}\text{O}_{61}]$ yielded a nonreactive intermediate species $\text{POM}-\text{Fe}^{\text{III}}-\text{OIAr}$ ($\text{Ar} = \text{Ph}$, F_5Ph), rather than a reactive $\text{POM}-\text{Fe}=\text{O}$ species. Use of iodosobenzene derivatives as oxidants in other iron-based systems has also shown formation of such $\text{Fe}^{\text{III}}-\text{OIAr}$ intermediates.²³ It should be noted that use of other strong monooxygen donors such *m*-chloroperbenzoic acid showed a Fenton type reactivity in the presence of ${}^4\text{Q}_7[\text{P}_2\text{Fe}^{\text{III}}(\text{H}_2\text{O})\text{W}_{17}\text{O}_{61}]$ rather than oxygen transfer.

Our gas-phase UB3LYP/B1 calculations, in Figure 6, reveal a tight complex formation between F_5PhI and $\text{POM}-\text{Fe}=\text{O}^{4-}$ with a binding energy of 20 kcal/mol, much higher than the binding energy of propene to the reagent (see, e.g., Figure 2). The use of single-point calculations with the SCRF model reduces the dissociation energy of the complex to 5.5 kcal/mol with $\epsilon = 5.7$, and with $\epsilon = 37.5$, the binding energy is further reduced (becoming -0.7 kcal/mol). The use of COSMO led to

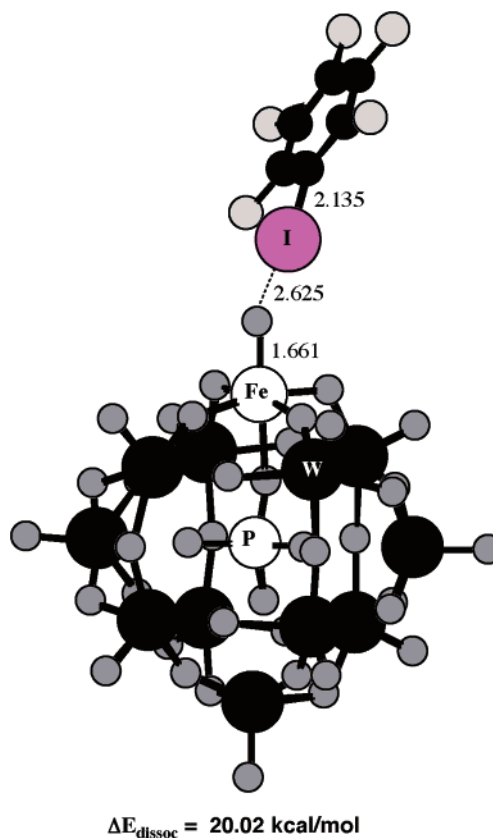


Figure 6. Key geometric features and gas-phase binding energy of the $\text{POM}-\text{Fe}^{\text{III}}-\text{O}-\text{I}(\text{F}_5\text{Ph})^{4-}$ complex, optimized by UB3LYP/B1 in the quartet state. The dissociation energy refers to the following process: $\text{POM}-\text{Fe}^{\text{III}}-\text{O}-\text{I}(\text{F}_5\text{Ph})^{4-} \rightarrow \text{POM}-\text{Fe}^{\text{III}}-\text{O}^{4-} + \text{F}_5\text{Ph}-\text{I}$.

similar results; the binding energy with $\epsilon = 37.5$ is -1.5 kcal/mol. Thus, it is clear that the solvent reduces the binding energy. However, be the precise binding energy value in a solvent as it may, the gas phase results reveal a tightly bound complex, and as such we may tentatively propose a physical mechanism for barrier formation.²⁴ Thus as the $\text{O}-\text{I}$ bond is stretched in a solvent, the intrinsic gas-phase energy curve will increase, while the solvation energy curve will be lowered, leading to a barrier that reflects the interplay of binding strength and solvent reorganization during the dissociation. As such, the $\text{POM}-\text{Fe}^{\text{III}}-\text{O}-\text{I}(\text{F}_5\text{Ph})^{4-}$ complex is going to be persistent, and at the same time, propene will not be able to displace the of F_5PhI molecule to form the encounter complex necessary for oxidation. These conclusions regarding the $\text{POM}-\text{Fe}^{\text{III}}-\text{O}-\text{I}(\text{F}_5\text{Ph})^{4-}$ complex are further supported by the NMR experiments, which indicate a persistent complex.

Discussion

The theoretical results of this study show that $\text{POM}-\text{FeO}^{4-}$ should be an extremely reactive iron-oxo species. The experimental and theoretical results reveal also that the apparent lack of reactivity, noted here and elsewhere,⁵ is due to the formation of a $\text{POM}-\text{FeO}-\text{I}(\text{F}_5\text{Ph})^{4-}$ complex that is persistent at the working conditions and exhibits sluggish reactivity if at all. The theoretical calculations show that the interaction between the ArI and $\text{POM}-\text{FeO}^{4-}$ moieties is 20 kcal/mol strong in the gas phase, and despite its expected weakening by solvation, it is likely to cause a barrier for dissociation.

(23) Nam, W.; Choi, S. K.; Lim, J. R.; Kim, I.; Kim, C.; Que, L., Jr. *Angew. Chem., Int. Ed.* **2003**, *42*, 109.

(24) Shaik, S.; Shurki, A. *Angew. Chem., Int. Ed.* **1999**, *38*, 586.

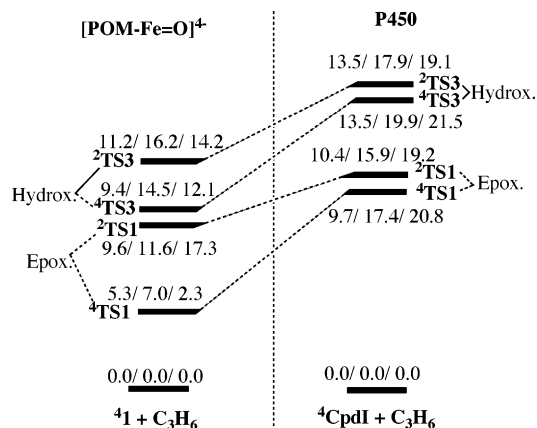


Figure 7. Bond activation barriers (in kcal/mol) for epoxidation (via **TS1**) and allylic hydroxylation (via **TS3**) of propene by POM-FeO⁴⁻ (**1**) and Compound I (Cpd I) of P450 (from ref 12). The data in is arranged as B1 energy/B2 energy + ε = 5.7/B2 energy + ε = 37.5.

Complexes of the general formula LFeO-IAr (L = macrocycle ligand, Ar = Aryl) type have been postulated by Collman et al.²⁵ and were recently detected for iron porphyrin (Por) complexes, by Nam et al.²³ who characterized the PorFeO-IPh complex by spectroscopic means. Nam et al.²³ demonstrated that PorFeO + PhI and PorFeO-IPh coexist in equilibrium and the equilibrium mixture is reactive; it was not possible, however, to compare separately the reactivity of the two oxidant species. Recently, Bhakta et al.²⁶ used iodosobenzene to generate the Compound I species of cytochrome P450. They observed that product distribution resulting from this experiment was different than the distribution resulting from the natural generation of Compound I (with O₂, NADPH) and postulated the formation of PorFeO-IPh, which reacts with the substrate in a manner different than Compound I. In our study, the POM-FeO-IPhF₅⁴⁻ species is experimentally unreactive or at best only slightly reactive. Our preliminary theoretical results show that the same complex with the POM-MnO-IPhF₅³⁻ has a significantly weaker binding energy, which may in part account for the experimental observations that the manganese reagent is reactive.⁵

Theory shows that if the POM-FeO-IAr⁴⁻ complex decomposes it will generate a highly potent POM-FeO⁴⁻ reagent. To appreciate this potency of POM-FeO⁴⁻ we present in Figure 7 the UB3LYP/B1 and UB3LYP/B2 barriers for C-H hydroxylation and C=C epoxidation as found in the present study, alongside the corresponding barriers for the same processes with the Compound I species of P450.¹² It is seen that the gas-phase barriers with POM-FeO⁴⁻ are significantly lower than those of P450 Compound I. Figure 8 shows that the reason for the lower gas-phase barriers of POM-FeO⁴⁻ is the interaction of the developing positive charge on the propene moiety with the negatively charged sphere of the POM lacunary. By contrast, Compound I of P450 is neutral and is hence devoid of the charge stabilization mechanism in the bond activation transition state. As further shown in Figure 7, an additional factor that makes POM-FeO⁴⁻ a potentially powerful oxidant is the effect of the

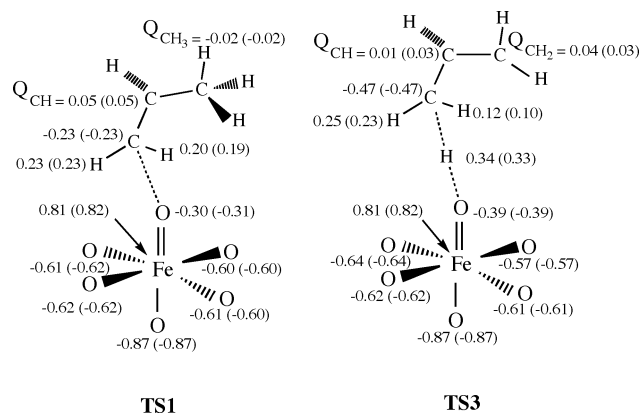


Figure 8. Charge distribution in **TS1** and **TS3**. The interactions between the positively charged propene moiety and the negatively charged Fe-(O)₆ moiety of POM-FeO stabilizes both transition states.

solvent. Thus, since the propene develops positive charge, in the transition state, this results in additional charging of the already negatively charged POM-FeO⁴⁻ moiety. Since classical solvation energy varies with the charge squared, the additional charging of the POM will cause further stabilization of the transition states for either the hydroxylation or epoxidation, and the respective barriers are lowered compared with those of P450 Compound I. Our calculations indicate that in a solvent, the barriers, and especially those for epoxidation, become sufficiently small that one may expect an extremely fast reaction. The question is, can POM-FeO⁴⁻ be made?

Conclusions

There is a continuing search for efficient and robust catalysts that can perform monooxygenation of organic compounds. This study identifies one such potential system based on iron-substituted polyoxometalate (POM-Fe). The POM system is robust and is a very good platform for generating reactive metal-oxo reagent.²⁷ Indeed, this study shows that POM-FeO⁴⁻ is a powerful oxidant, even more so than P450, capable of C-H hydroxylation and C=C epoxidation. Unfortunately, the formation of POM-FeO⁴⁻ using the usual oxygen atom surrogate, F₅PhI-O, leads to a persistent adduct, POM-FeO-I-PhF₅⁴⁻ (see Figure 6), which exhibits sluggish reactivity. There must be a way to overcome this technical difficulty. According to theory, such a way may turn out to be very rewarding.

Acknowledgment. This research was supported by the German Federal Ministry of Education and Research (BMBF) within the framework of the German-Israeli Project Cooperation (DIP). R.N. is the Rebecca and Israel Sieff Professor of Organic Chemistry.

Supporting Information Available: Reference 16a in full, 24 tables, and 16 figures with structures and profiles (PDF). This material is available free of charge via the Internet at <http://pubs.acs.org>.

JA0542340

(25) Collman, J. P.; Chien, A. S.; Eberspacher, T. A.; Brauman, J. I. *J. Am. Chem. Soc.* **2000**, *122*, 11098.

(26) Bhakta, M. N.; Hollenberg, P. F.; Wimalasena, K. *J. Am. Chem. Soc.* **2005**, *127*, 1376.

(27) Recent electrospray ionization and Fourier transform ion cyclotron spectrometric techniques show that it is possible to prepare Cpd I type species of heme complexes in the gas phase and gauge their reactivity. See: Crestoni, M. E.; Fornarini, S. *Inorg. Chem.* **2005**, *15*, 5379.